



# Nickelalumite, ideally $\text{NiAl}_4(\text{SO}_4)(\text{OH})_{12}(\text{H}_2\text{O})_3$ , a new-old mineral from the Kara-Tangi uranium deposit, Kyrgyzstan

Vladimir Yu. Karpenko<sup>1</sup> · Atali A. Agakhanov<sup>1</sup> · Leonid A. Pautov<sup>1,2</sup> · Galiya K. Bekenova<sup>3</sup> · Yulia A. Uvarova<sup>4</sup> · Elena Sokolova<sup>5</sup> · Tamara V. Dikaya<sup>1</sup> · Frank C. Hawthorne<sup>5</sup>

Received: 4 January 2023 / Accepted: 2 May 2023 / Published online: 2 June 2023  
© The Author(s), under exclusive licence to Springer-Verlag GmbH Austria, part of Springer Nature 2023

## Abstract

Nickelalumite, ideally  $\text{NiAl}_4(\text{SO}_4)(\text{OH})_{12}(\text{H}_2\text{O})_3$ , is a newly approved mineral from the Batken region, Kyrgyzstan, where it occurs in the Kara-Tangi and Kara-Chagyir uranium deposits. It formed in a zone of hydrothermal alteration of U–V-bearing carbonaceous siliceous schists, in association with quartz, calcite, alumohydrocalcite, allophane, crandallite, kyrgyzstanite, ankinovichite and an unknown Al–OH-mineral. It occurs as aggregates of colourless to pistachio-green radiating bladed crystals from 0.05 to 0.50 mm long. It is vitreous to transparent in thin flakes, has a white streak, and shows no fluorescence under long-wave or short-wave ultraviolet light. Cleavage is perfect parallel to {001} and no parting was observed. Mohs hardness is 2, it is brittle and has a splintery fracture. The calculated mass density is  $2.231 \text{ g cm}^{-3}$ . In transmitted plane-polarized white light, nickelalumite is non-pleochroic, biaxial,  $\alpha = 1.542(2)$ ,  $\gamma = 1.533(2)$ ,  $\beta$  could not be measured due to the almost negligible thickness of the flakes. EPMA chemical analysis gave  $\text{Al}_2\text{O}_3$  39.94,  $\text{SiO}_2$  0.17,  $\text{SO}_3$  15.20,  $\text{V}_2\text{O}_5$  0.29,  $\text{FeO}$  0.15,  $\text{NiO}$  8.00,  $\text{ZnO}$  6.21,  $(\text{H}_2\text{O})_{\text{calc}}$  31.87, total 101.83 wt%,  $\text{H}_2\text{O}$  was determined by crystal-structure analysis, and the empirical formula is as follows:  $(\text{Ni}_{0.55}\text{Zn}_{0.39}\text{V}_{0.02}\text{Fe}_{0.01})_{\Sigma 0.97}(\text{Al}_{3.99}\text{Si}_{0.01})_{\Sigma 4.00}(\text{SO}_4)(\text{OH})_{12}(\text{H}_2\text{O})_3$  based on 4 (Al + Si) cations. There is considerable variation in substitution of Zn, Cu, Fe and  $\text{V}^{3+}$  for Ni and  $\text{V}^{3+}$  for  $\text{S}^{6+}$ . Nickelalumite is monoclinic,  $P2_1/n$ ,  $a = 10.2567(5)$ ,  $b = 8.8815(4)$ ,  $c = 17.0989(8)$  Å,  $\beta = 95.548(1)^\circ$ ,  $V = 1550.3(2)$  Å<sup>3</sup>,  $Z = 4$ . The crystal structure of nickelalumite was refined to an  $R_1$  index of 5.66% and consists of interrupted  $[\text{NiAl}_4(\text{OH})_{12}]$  sheets intercalated with layers of  $\{(\text{SO}_4)_2(\text{H}_2\text{O})_3\}$ ; nickelalumite is a member of the chalcoalumite group.

**Keywords** Nickelalumite · New mineral species · Sulfate · Crystal structure · EPMA chemical analysis · Chalcoalumite group V-bearing schists · Kara-Tangi

## Introduction

Nickelalumite,  $(\text{Ni}_{0.75}\text{Cu}_{0.25})_{\Sigma 1.00}\text{Al}_4[\text{SO}_4]_{\Sigma 0.75}(\text{NO}_3)_{\Sigma 0.50}(\text{OH})_{12}(\text{H}_2\text{O})_3$ , was first described from the Mbobo Mkulu cave, Nelspruit district, eastern Transvaal, together with two other minerals: mbobomkulite,  $(\text{Ni}, \text{Cu}^{2+})\text{Al}_4[(\text{NO}_3), (\text{SO}_4)]_2(\text{OH})_{12}(\text{H}_2\text{O})_3$ , and hydrombobomkulite,  $(\text{Ni}, \text{Cu}^{2+})\text{Al}_4[(\text{NO}_3), (\text{SO}_4)]_2(\text{OH})_{12}(\text{H}_2\text{O})_{12}$  (Martini 1980). Mbobomkulite and hydrombobomkulite were approved by IMA (International Mineralogical Association)-CNMMN (Commission on New Minerals and Mineral Names) but nickelalumite was rejected because of some problems with chemical composition (Jacques Martini, personal communication). Nickelalumite was stated to be the nickel analogue of chalcoalumite,  $\text{CuAl}_4(\text{SO}_4)(\text{OH})_{12}(\text{H}_2\text{O})_3$ ,  $a$  17.090 Å,  $b$  8.915 Å,  $c$  10.221 Å,  $\beta$  95.88°, space group  $P2_1$  (Larsen and Vassar 1925; Williams and Khin 1971).

Editorial handling: M. Wildner

✉ Frank C. Hawthorne  
frank.hawthorne@umanitoba.ca

- <sup>1</sup> A.E. Fersman Mineralogical Museum, Russian Academy of Sciences, Moscow 117071, Russia
- <sup>2</sup> South Urals Federal Research Center of Mineralogy and Geoecology UB RAS, Institute of Mineralogy, Chelyabinsk Region, Miass 456317, Russia
- <sup>3</sup> Satpaev Institute of Geological Sciences, ul. Kabanbai batyr 69, Almaty 050010, Kazakhstan
- <sup>4</sup> CSIRO Mineral Resources, ARRC, 29 Dick Perry Avenue, Kensington, Western Australia 6151, Australia
- <sup>5</sup> Department of Earth Sciences, University of Manitoba, Winnipeg, Manitoba R3T 2N2, Canada

During investigation of vanadium-bearing schists from Kyrgyzstan, we found nickelalumite as a constituent of crystalline crusts at Kara-Chagyr and Kara-Tangi (Karpenko et al. 2004a). The nickelalumite crystals at the Kara-Tangi are of reasonable quality and allowed the structure of the mineral to be refined (Uvarova et al. 2005) and properties to be measured accurately. Thus we chose Kara-Tangi as the type locality for nickelalumite which has been approved as a new mineral species by the IMA-CNMNC (Commission on New Minerals, Nomenclature and Classification), 2022-071. Dr. Martini declined to participate in the IMA approval procedure, stating that he is now out of mineralogy; however, he welcomed our initiative to formalize the mineral. Here we describe nickelalumite from all three localities. The holotype sample from Kara-Tangi is deposited in the systematic collection (# 98105) at the A.E. Fersman Mineralogical Museum, Moscow, Russia.

## Occurrence

In the southern part of the Fergana valley, a belt of outcrops of black carbonaceous schists extends for 100 km along the foothills of the Alai range. The schists are part of the South Fergana mélangé involving large blocks of Early Paleozoic carbonaceous siliceous rocks in a matrix of serpentinite. Initially investigated by Scherbakov (1924), Preobrazhensky (1926) and many others, the schists contain extensive U-Ni-Zn-V mineralization. The most significant exposures are at Kara-Tangi and Kara-Chagyr in the Batken region, Kyrgyzstan (Karpenko et al. 2004a) and show extensive Ni-Zn-V mineralization (Agakhanov et al. 2005; Karpenko et al. 2004a, b, 2009, 2011, 2016), and nickelalumite was found at both these localities. At Kara-Tangi, there is a minor U-deposit that was worked in the 1960–1970s (V. Rogovoy, personal communication) and is located in a

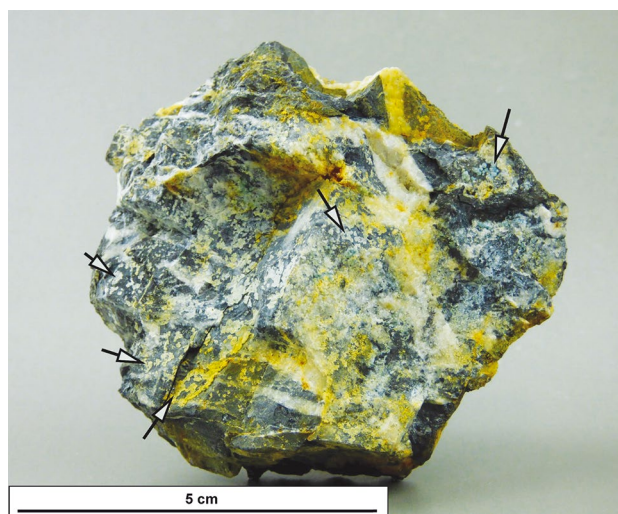


**Fig. 2** A typical hand-specimen (6.0 cm × 7.5 cm) of carbonaceous U–V-bearing black schist (black), penetrated by quartz veins and covered with very light greenish-bluish crystalline crust mainly of nickelalumite and kyrgyzstanite, Kara-Tangi dumps. Arrows show typical aggregations of nickelalumite and kyrgyzstanite, which are widespread on the surface of the specimen. Their hue is sometimes yellowish (bottom arrow) because of Fe-secondary oxides

gorge (Fig. 1a) with the same name on the northern slope of the Katran-Tau mountains, Batken region, Kyrgyzstan. The deposit occurs in a zone of strongly folded chlorite-sericite slates (Fig. 1b) of Upper-Silurian age, and the mineralization occurs in boudinaged carboniferous black schists. The size of the lenses ranges from one metre to several tens of metres in length.

Nickelalumite was found on the surface of carbonaceous siliceous schist in the dumps of the mine adit on the right side of Kara-Tangi gorge (GPS coordinates 40° 07' 09" N, 71° 17' 50" E). It forms pale-blue to greenish crusts of radiating lamellar aggregates of crystals up to 1.5 mm,

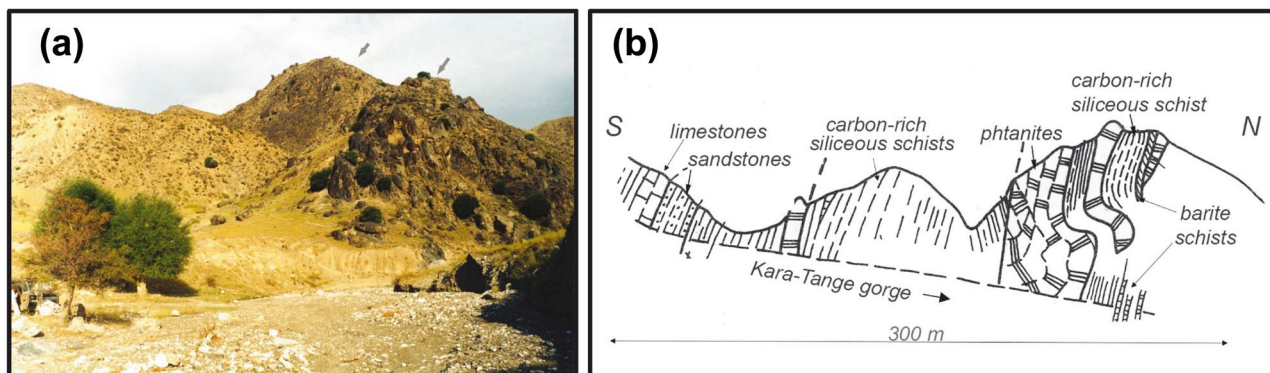
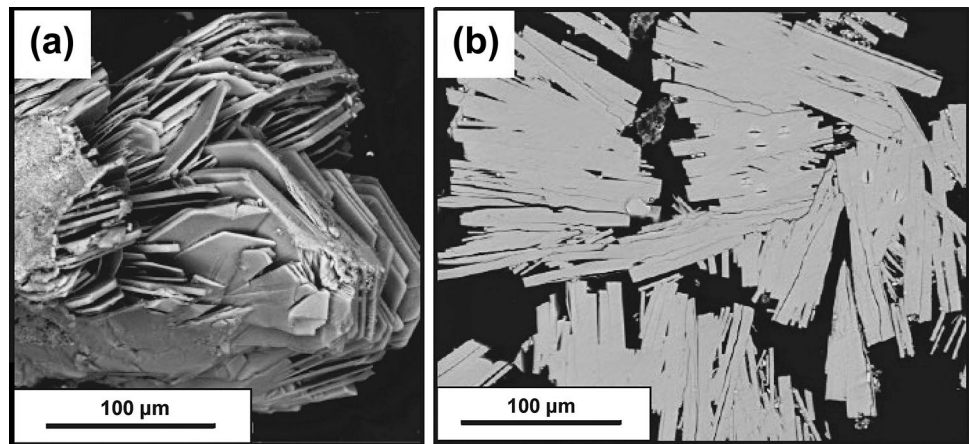


**Fig. 1** The Kara-Tangi deposit: (a) a view of the deposit; the locations of the blocks of black schist mined for uranium are indicated by black arrows; (b) sketch of the geology across the Kara-Tangi valley (from Porshnyakov et al. 1991)

**Fig. 3** An aggregation of lamellar split crystals of nickelalumite from Kara-Tangi: (a) secondary electron image of the unprepared specimen; (b) polished section in BSE mode. Photos by Ilya B. Afanasyev



and also occurs in cracks and small cavities (Fig. 2) associated with quartz, calcite, alumohydrocalcite, kyrgyzstanite, ankinovichite and boehmite. Some aggregates are replaced by allophane. Nickelalumite crystals are lamellar and split (Fig. 3a, b), and resemble kyrgyzstanite, the zincian analogue of nickelalumite (Agakhanov et al. 2005).

At Kara-Chagyr, nickelalumite occurs as crusts of radiating fibrous aggregates up to 1.5 mm which are commonly intercalated with allophane and are closely associated with ankinovichite, Zn-Ni-bearing volborthite, allophane, tyuyamunite and rare tangeite (Fig. 4a). In cavities in the rock, it can form almost ideal spheres up to 1.5 mm in diameter growing on lamellar skeletal crystals of volborthite (Fig. 4b). Here, nickelalumite shows complex zoning (Fig. 4c, d), and for this reason, nickelalumite from Kara-Tangi was chosen as the holotype material.

## Analytical characterization

### Physical properties

Nickelalumite occurs as aggregates of radiating bladed crystals from 0.05 to 0.50 mm long (Fig. 3); individual crystals disaggregate into fibres and flakes that deform under the slightest touch. Colour varies from almost colourless through light blue to pistachio green depending on crystal size and V content. Nickelalumite is vitreous to transparent in thin crystals, has a white streak, and shows no fluorescence under long-wave or short-wave ultraviolet light. Cleavage is perfect parallel to  $\{001\}$  and no parting was observed. Mohs hardness is 2, it is brittle and has a splintery fracture. The calculated mass density is  $2.231 \text{ g cm}^{-3}$  and it is soluble in hot (1:1) HCl.

**Fig. 4** Spherulite aggregations of nickelalumite from Kara-Chagyr: (a) ankinovichite (Ank) overgrowth on nickelalumite (Nick); (b) spherulites of V-bearing nickelalumite covered with volborthite (Volb); (c) BSE image of cross-cut ankinovichite (ank) – nickelalumite (nick) crust with kaolinite (kaol); (d) BSE image of cross-cut of nickelalumite (1) and Si-V-rich nickelalumite (2) as part of the complex zoned spherulite; frame shows area covered by images in Fig. 7. White-light photographs (a) and (b) by Natalya A. Pekova

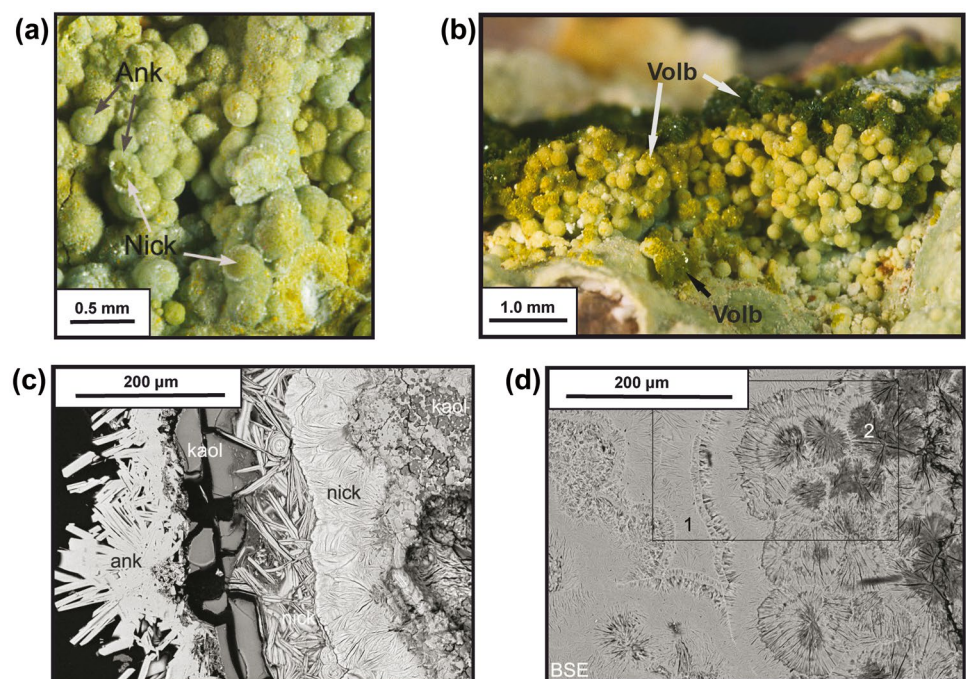
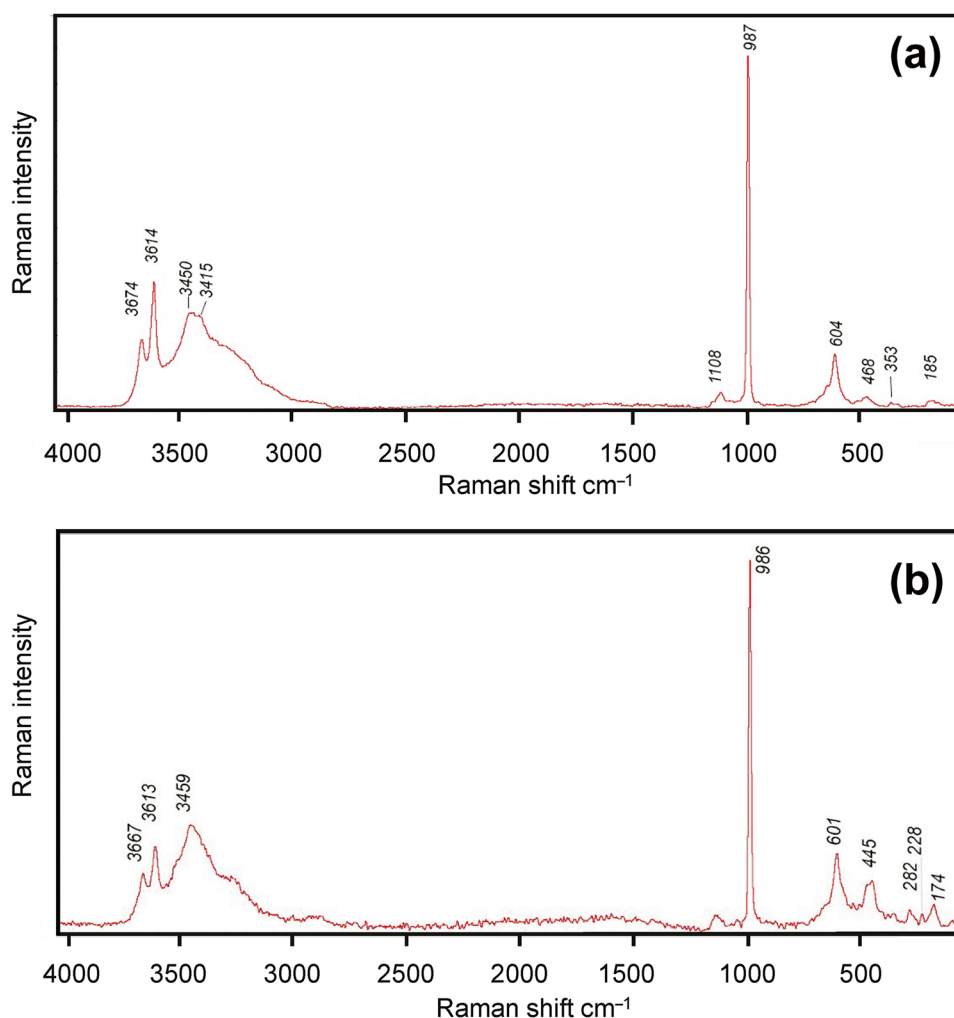


**Fig. 5** Raman spectra of nickelalumite: (a) Kara-Tangi, Kyrgyzstan; (b) Mbobo Mkulu, R.S.A



In transmitted plane-polarized white light, nickelalumite is non-pleochroic. A spindle stage was used to orient a crystal for measurement of refractive indices in white light (Bartelmehs et al. 1992). Nickelalumite is biaxial,  $\alpha = 1.542(2)$ ,  $\gamma = 1.533(2)$ ,  $\beta$  could not be measured due to the almost negligible thickness of the flakes. Extinction is oblique ( $\sim 40^\circ$ ). The average refractive index for vanadium-bearing nickelalumite ( $V_2O_5$  6.0 wt%) from Kara-Chagyr is  $\sim 1.575$ – $1.580$ , in accord with the refractive indices of ankinovichite, the vanadium analogue of nickelalumite (Karpenko et al. 2004a, b).

### Raman spectroscopy

The Raman spectrum of nickelalumite from Kara-Tangi (Fig. 5a) was obtained at room temperature on a polished crystal using a Thermo DXR2xi Raman imaging confocal microscope with a green laser (532 nm). The output power of the laser beam was 8 mW (at 80% power), the holographic diffraction grating had 400 lines  $cm^{-1}$ , and the spectral resolution was 2  $cm^{-1}$ . The diameter of the focal spot on the sample

was 2  $\mu m$ . The backscattered Raman signal was collected with a 100 $\times$  objective; signal-acquisition time for a single scan of the spectral range was 0.3 s and the signal was averaged over 30 scans. The spectrum was processed using Omnic software. Two sharp lines at 3674 and 3614  $cm^{-1}$  correspond to (OH)-stretching. There are two distinct (OH) groups in the structure: (1) those where the donor O bonds to two  $[6]Al$ , and (2) those where the donor O bonds to two  $[6]Al$  plus  $[6]Zn$ . The latter will have stronger hydrogen bonding resulting in lower stretching frequency, and hence will occur at lower Raman shift: 3614  $cm^{-1}$ . There is a broad absorption in the range 2800–3500  $cm^{-1}$  that corresponds to ( $H_2O$ ) stretching. An intense band at 987  $cm^{-1}$  and a weak band at 1108  $cm^{-1}$  correspond to the  $\nu_1$  symmetric and  $\nu_3$  antisymmetric stretching of the ( $SO_4$ ) tetrahedra; the band at 604  $cm^{-1}$  corresponds to bending vibrations of ( $SO_4$ ); and the weak band at 468  $cm^{-1}$  is associated with ( $SO_4$ ) and ( $AlO_6$ ) bending modes. A similar spectrum was obtained from tiny flakes of nickelalumite (sample #MGS 18211) obtained from the National Museum of Natural History, Pretoria, Republic of South Africa, Council for Geoscience, South Africa (Fig. 5b).

**Table 1** Chemical composition (wt%) for nickelalumite (1–4) and kyrgyzstanite (5)

Components	1	2	3	4	5
Al <sub>2</sub> O <sub>3</sub>	39.3	41.65	39.94	38.99–40.63	38.45
V <sub>2</sub> O <sub>3</sub>	–	–	0.29	0.11–0.40	0.06
SiO <sub>2</sub>	8.95	–	0.17	0.11–0.23	0.33
SO <sub>3</sub>	10.28	13.53	15.2	14.82–15.56	15.00
NiO	6.59	10.08	8.00	7.54–8.62	4.13
ZnO	n.d.	n.d.	6.21	5.73–6.88	10.02
CuO	2.35	0.93	n.d.		0.58
FeO	–	–	0.15	0.04–0.25	0.32
N <sub>2</sub> O <sub>5</sub>	4.70	–	n.d.		0.00
C	<0.30	–	n.d.		n.d.
H <sub>2</sub> O	28.53	–	31.87		30.10
Total	100.7		101.83		98.99

1, 2: Mbobu Mkuku, R.S.A. (Martini 1980) (1: blue nodules in allophane, wet chemistry; 2: crust on gypsum, microprobe); 3, 4: nickelalumite, used for crystal-structure refinement, Kara-Tangi, Kyrgyzstan, our data (3: average from 10 microprobe analyses; 4: range of composition); 5: kyrgyzstanite, Kara-Tangi, Kyrgyzstan, average from 6 microprobe analyses (Agakhanov et al. 2005)

Empirical formulae:

1: (Ni<sub>0.75</sub>Cu<sub>0.25</sub>)<sub>Σ1.00</sub>Al<sub>4</sub>[SO<sub>4</sub>]<sub>Σ0.75</sub>(NO<sub>3</sub>)<sub>Σ0.50</sub>(OH)<sub>12</sub>(H<sub>2</sub>O)<sub>3</sub> (Martini 1980)

3: (Ni<sub>0.55</sub>Zn<sub>0.39</sub>V<sub>0.02</sub>Fe<sub>0.01</sub>)<sub>Σ0.97</sub>(Al<sub>3.99</sub>Si<sub>0.01</sub>)<sub>Σ4.00</sub>(SO<sub>4</sub>)(OH)<sub>12</sub>(H<sub>2</sub>O)<sub>3</sub> (Agakhanov et al. 2005)

## Chemical composition

In order to understand why nickelalumite was not approved originally by IMA-CNMMN, we examined powder sample #MGS 18211 in BSE (back-scattered electron) mode. It consists of thin plates of pure nickelalumite mixed with Al–Si-rich material, probably allophane (Martini 1980), that resulted in excess Si in the formula.

The original analysis of nickelalumite from Mbobu Mkulu, South Africa (Martini 1980) (analysis 1, Table 1) included 4.70 wt% N<sub>2</sub>O<sub>5</sub> and a deficiency in S (0.75 *apfu*, atoms per formula unit), suggesting replacement of (SO<sub>4</sub>)<sup>2-</sup> by (NO<sub>3</sub>)<sup>2-</sup>. In this regard, Williams et al. (2011) reported the synthesis of ZnAl<sub>4</sub>(NO<sub>3</sub>)<sub>2</sub>(OH)<sub>12</sub>(H<sub>2</sub>O)<sub>x</sub> with highly disordered interlayer (NO<sub>3</sub>)<sup>-</sup> oxyanions. They dehydrated their disordered material to [ZnAl<sub>4</sub>(OH)<sub>12</sub>](NO<sub>3</sub>)<sub>2</sub> and showed that the structure contains [ZnAl<sub>4</sub>(OH)<sub>12</sub>] layers topologically the same as those in nickelalumite, supporting the idea that (NO<sub>3</sub>)<sup>2-</sup> may replace (SO<sub>4</sub>)<sup>2-</sup> in the nickelalumite structure.

The composition of nickelalumite was obtained for the crystal used for X-ray diffraction. It was mounted on a Perspex disc, ground, polished, carbon-coated and analyzed with a Cameca SX 100 electron probe micro-analyser (EPMA) operating in wavelength-dispersion mode with an accelerating voltage of 15 kV, a specimen current of 3 nA, a beam size of 20 μm and counting times on peak and background of 20 and 10 s, respectively.

**Table 2** Chemical composition (EPMA results) and calculated mineral formulae for nickelalumite

Component	1	2	3	4	5	6	7	8	9	10	11	12	13	14
Major oxides (wt%)														
Al <sub>2</sub> O <sub>3</sub>	39.24	39.54	37.36	38.59	37.76	37.67	37.73	38.83	38.05	36.35	38.99	38.77	38.01	39.02
V <sub>2</sub> O <sub>3</sub>	0.40	0.52	0.78	0.68	0.00	0.17	0.09	0.00	0.00	4.42	4.59	4.15	8.06	7.18
SiO <sub>2</sub>	0.15	0.00	0.00	0.00	0.38	0.41	0.64	0.69	0.77	1.08	0.61	1.10	3.79	1.33
SO <sub>3</sub>	15.71	16.07	15.67	16.18	14.38	14.11	14.54	14.80	14.45	11.99	13.10	11.96	9.46	11.83
NiO	9.06	11.01	11.50	10.45	7.05	9.87	8.08	10.03	12.07	10.03	8.87	7.77	10.81	9.90
ZnO	5.12	3.86	3.50	3.93	6.64	4.88	6.24	4.83	0.66	1.15	0.34	2.25	2.86	1.46
CuO	0.00	0.00	0.00	0.00	0.72	0.10	0.52	0.22	0.00	1.10	0.31	0.95	2.21	1.92
FeO	0.00	0.00	0.00	0.00	0.00	0.29	0.33	0.00	0.00	0.00	0.00	1.80	0.00	0.42
Total	69.68	71.00	68.81	69.83	66.93	67.50	68.17	69.40	66.00	66.12	66.81	68.75	75.20	73.06
Calculated mineral formulae* ( <i>apfu</i> )														
Ni <sup>+2</sup>	0.63	0.75	0.81	0.73	0.51	0.71	0.57	0.70	0.87	0.73	0.63	0.54	0.71	0.67
Zn <sup>+2</sup>	0.33	0.24	0.23	0.25	0.44	0.32	0.41	0.31	0.04	0.08	0.02	0.14	0.17	0.09
Cu <sup>+2</sup>	0.00	0.00	0.00	0.00	0.05	0.01	0.03	0.01	0.00	0.08	0.02	0.06	0.14	0.12
Fe <sup>+2</sup>	0.00	0.00	0.00	0.00	0.00	0.02	0.02	0.00	0.00	0.82	0.00	0.13	0.00	0.03
V <sup>+3</sup>	0.03	0.04	0.05	0.05	0.00	0.01	0.01	0.00	0.00	0.32	0.33	0.29	0.43	0.40
Al <sup>+3</sup>	3.99	3.95	3.87	3.93	4.00	3.95	3.93	3.96	4.03	3.88	4.07	3.96	3.65	3.85
Si <sup>+4</sup>	0.01	0.00	0.00	0.00	0.03	0.04	0.06	0.06	0.07	0.10	0.05	0.10	0.31	0.11
S <sup>+6</sup>	1.02	1.02	1.03	1.05	0.97	0.94	0.96	0.96	0.98	0.82	0.87	0.78	0.58	0.74

1–8: nickelalumite, Kara-Tangi (light-blue radiate-fibrous segregations); 9–14: nickelalumite, Kara-Chagyr (9: light-blue needle-shaped, 10–12: light-green spherulites of V-bearing nickelalumite; 13, 14: dark-green spherulites of high-vanadium nickelalumite); 1–4, 13, 14: our data; 5–12: Karpenko et al. (2004a)

\* Calculated based on 6 (Ni + Zn + Cu + Fe + V + Al + Si + S) atoms per formula unit

**Fig. 6** Compositional variation in nickelalumite from Kara-Tangi (green circles), Kara-Chagyr (brown circles) and Mbobbo Mkulu (large brown triangle); the red diamond is the end-member composition of nickelalumite; (a) (Zn + Cu + Fe) versus Ni; the pale-blue diamond is the end-member composition of kyrgyzstanite and the yellow star is the composition of the crystal structure refined here; (b) V versus S; the dark-blue diamond is the end-member composition of ankinovichite

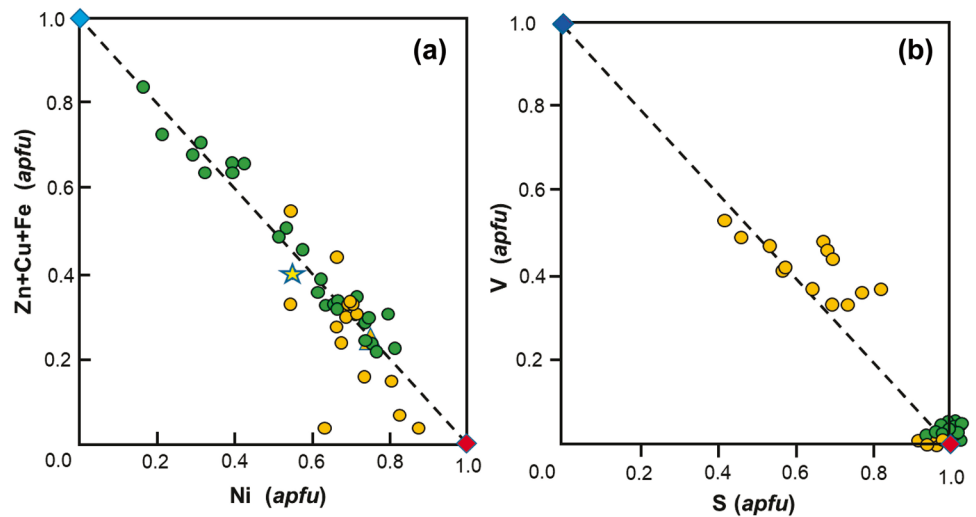


**Fig. 7** X-ray maps of the area in the frame on Fig. 4d

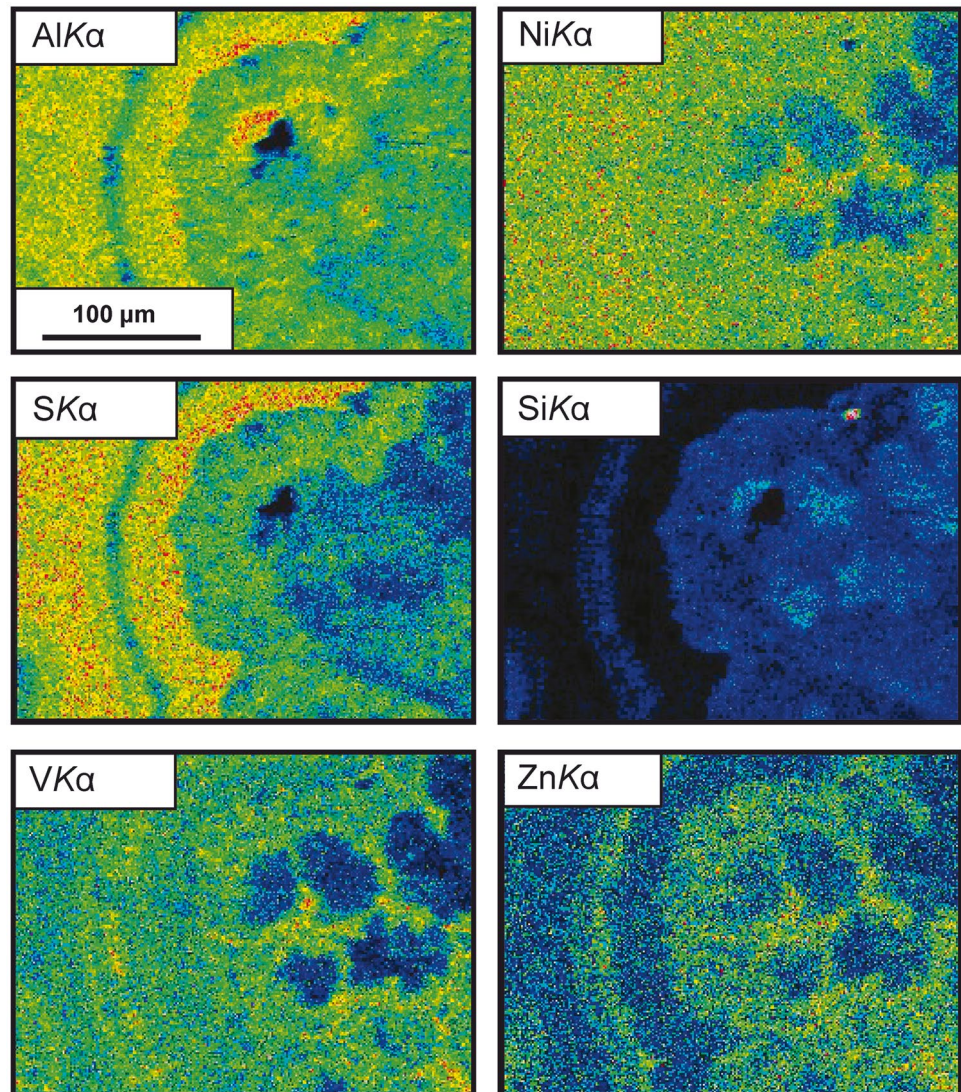


**Table 3** X-ray powder-diffraction pattern for nickelalumite

<i>I</i>	<i>d</i> <sub>obs</sub> (Å)	<i>d</i> <sub>calc</sub> (Å)	<i>h k l</i>
10	8.35	8.515	0 0 2
3	6.67	6.684	1 1 0
3	4.62	4.556	2 0 -2
9	4.27	4.258	0 0 4
2	3.71	3.693	1 1 -4
5	3.30	3.317	2 2 -1
4	3.16	3.177, 3.179	2 2 -2, 0 1 5
6	3.02	3.049	2 2 2
6	2.683	2.701	0 2 5
2	2.592	2.598	2 1 5
8	2.508	2.501, 2.510	4 0 -2, 2 3 1
7	2.276	2.291, 2.278	2 3 3, 4 0 -4
3	2.222	2.216	0 4 0
2	2.067	2.065	1 1 -8
9	1.981	1.987	4 0 -6
3	1.824	1.823	5 2 1
3	1.811	1.814	4 0 6
4	1.740	1.740	1 2 -9
4	1.710	1.712	4 0 -8
1	1.647	1.653	4 1 7
3	1.556	1.555	2 3 -9
6	1.480	1.476	6 3 -1
6	1.455	1.456, 1.456	6 3 1, 0 6 2
4	1.400	1.397	6 3 3
4	1.361	1.359	4 0 10
1	1.302	1.306, 1.298	6 3 -7, 2 3 11
1	1.272	1.272, 1.272	8 0 0, 4 6 -2
1	1.241	1.239, 1.242	4 6 -4, 8 0 2
1	1.217	1.216	0 0 14
4	1.189	1.189, 1.188	8 0 4, 2 3 -13

$a = 10.219(10)$  Å,  $b = 8.863(12)$  Å,  $c = 17.103(15)$  Å,  $\beta = 95.26(10)^\circ$

$V = 1543(2)$  Å<sup>3</sup>

The following reference materials and crystals were used for *K* X-ray lines: Al: andalusite; Si: titanite; S: anhydrite; V: VP<sub>2</sub>O<sub>7</sub>; Ni: Ni<sub>2</sub>Si; Zn: gahnite; Fe: fayalite; Cu: CuFeS<sub>2</sub>. Data were reduced using the  $\Phi(\rho z)$  procedure (Merlet 1992). The amount of H<sub>2</sub>O was derived from structure refinement. Table 1 gives the chemical composition and empirical formula unit based on 4 (Al + Si) cations: (Ni<sub>0.55</sub>Zn<sub>0.39</sub>V<sub>0.02</sub>Fe<sub>0.01</sub>)<sub>Σ0.97</sub>(Al<sub>3.99</sub>Si<sub>0.01</sub>)<sub>Σ4.00</sub>[SO<sub>4</sub>](OH)<sub>12</sub>(H<sub>2</sub>O)<sub>3</sub>. The composition of kyrgyzstanite, a Zn-analogue of nickelalumite, is given for comparison (analysis 5, Table 1).

Variation in chemical composition of nickelalumite at both Kara-Tangi and Kara-Chagyr was examined with Jeol Superprobe 733 and JXA-50A electron probe micro-analyser equipped with Link energy-dispersive spectrometers. The experimental conditions for the Jeol Superprobe 733 were: accelerating voltage 20 kV, specimen current  $1 \times 10^{-9}$  A, reference materials Al<sub>2</sub>O<sub>3</sub> (Al), ZnS (S), magnetite USNM

**Table 4** Miscellaneous refinement data for nickelalumite

<i>a</i> (Å)	10.2567(5)
<i>b</i> (Å)	8.8815(4)
<i>c</i> (Å)	17.0989(8)
$\beta$ (°)	95.548(1)
<i>V</i> (Å <sup>3</sup> )	1550.3(2)
Space group	<i>P</i> 2 <sub>1</sub> / <i>n</i>
<i>Z</i>	4
Absorption coefficient (mm <sup>-1</sup> )	1.71
<i>F</i> (000)	1064.0
<i>D</i> <sub>calc.</sub> (g cm <sup>-3</sup> )	2.231
Crystal size	0.10 mm × 0.06 mm × 0.02 mm
Radiation/filter	MoK $\alpha$ /graphite
2 $\theta$ -range for data collection (°)	44.42
<i>R</i> (int) (%)	2.82
Reflections collected	26624
Unique reflections	15173
Independent reflections	1959
$F_o > 4\sigma F$	1554
Refinement method	Full-matrix least squares on <i>F</i> <sup>2</sup> , fixed weights proportional to $1/\sigma F_o^2$
Goodness of fit on <i>F</i> <sup>2</sup>	1.059
Final <i>R</i> <sub>(obs)</sub> (%)	<i>R</i> 1 = 5.66
[ $F_o > 4\sigma F$ ]	
<i>R</i> indices (all data) (%)	<i>R</i> 1 = 7.04 <i>wR</i> 2 = 16.72 Go <i>F</i> = 1.054

(Fe), metallic V and Cu (V, Cu), NiO (Ni), quartz (Si). Experimental conditions for the JXA-50A instrument were: accelerating voltage 20 kV, specimen current  $3 \times 10^{-9}$  A; for calibration microcline USNM 143966 (Si, Al), ilmenite USNM 96189 (Fe), gahnite USNM 145883 (Zn), metallic V and Cu (V, Cu), NiO (Ni), baryte (S) were used. The three USNM materials are Smithsonian “microbeam standards” (Jarosewich 2002). Following ZAF corrections, formulae were calculated based on 6 (Ni + Zn + Cu + Fe + V + Al + Si + S) *apfu* and are given in Table 2.

Variation in Ni content is linear with (Zn + Cu + Fe) content (Fig. 6a). The data for Kara-Tangi fall almost exactly along the line (Ni + Zn + Cu + Fe) = 1 *apfu* and show isomorphism between Ni and Zn, which leads to the nickelalumite–kyrgyzstanite series. The data for Kara-Chagyr are slightly displaced below the line, suggesting that there is an additional element at the Ni site in Kara-Tangi nickelalumite. In the interlayer, V shows an inverse linear correlation with S (Fig. 6b), primarily in the Kara-Chagyr samples, and there is a positive correlation between the intensity of (green) colour and the V content. It is possible that incorporation of some V<sup>3+</sup> could also occur at the Ni site *via* the substitution (VO<sub>4</sub>)<sup>3-</sup> + V<sup>3+</sup> → (SO<sub>4</sub>)<sup>2-</sup> + Ni<sup>2+</sup> which would account for

**Table 5** Hydrogen bonding in the crystal structure of nickelalumite

D – H...A	D – A (Å)	D – H (Å)	H – A (Å)	$\angle$ D – H...A (°)
*W(1)–H(1)–O(16)	2.926(5)	0.98(1)	2.03(1)	151.4(6)
W(1)–H(1)–O(14)	3.277(4)	0.98(1)	2.67(1)	139.9(1)
W(1)–H(2)–O(14)	2.863(4)	0.98(1)	1.89(1)	174.5(5)
W(1)–H(2)–O(13)	3.406(4)	0.98(1)	2.80(1)	120.7(5)
W(2)–H(3)–O(15)	2.870(5)	0.99(3)	1.95(1)	154.1(4)
W(2)–H(3)–O(13)	3.442(5)	0.99(3)	2.68(1)	134.2(4)
W(2)–H(4)–O(15)	2.958(4)	0.97(2)	2.03(1)	158.9(4)
W(3)–H(5)–O(16)	2.869(5)	0.98(1)	1.91(1)	163.8(5)
W(3)–H(5)–O(15)	3.294(4)	0.98(1)	2.65(1)	123.5(1)
W(3)–H(6)–W(1)	2.805(4)	0.98(1)	1.86(1)	162.8(1)
$\angle$ H(1)–W(1)–H(2)				109.1(1.7)
$\angle$ H(3)–W(2)–H(4)				110.7(3.0)
$\angle$ H(5)–W(3)–H(6)				109.4(1.8)
O(1)–H(7)–W(2)	2.822(5)	0.99(1)	1.88(1)	157.7(1)
O(2)–H(8)–O(14)	2.625(5)	0.99(1)	1.70(1)	153.6(1)
O(3)–H(9)–W(1)	2.765(4)	0.99(1)	1.79(1)	170.2(1)
O(4)–H(10)–W(2)	2.837(4)	0.99(1)	2.04(1)	137.1(1)
O(5)–H(11)–W(3)	2.998(5)	0.99(1)	2.02(1)	168.9(1)
O(6)–H(12)–W(3)	2.858(4)	0.99(1)	1.93(1)	156.6(1)
O(7)–H(13)–O(16)	2.782(4)	0.99(1)	1.81(1)	169.5(1)
O(8)–H(14)–O(15)	2.707(5)	0.99(1)	1.72(1)	174.0(1)
O(9)–H(15)–W(3)	2.944(5)	0.99(1)	1.98(1)	165.6(1)
O(10)–H(16)–O(13)	2.904(3)	0.99(1)	1.94(1)	164.1(1)
O(11)–H(17)–O(13)	2.698(4)	0.99(1)	1.73(1)	166.2(1)
O(12)–H(18)–O(13)	2.762(5)	0.99(1)	1.82(1)	157.4(1)

\* W: oxygen atom of an (H<sub>2</sub>O) group

the displacement of most of the Kara-Chagyr samples below the line in Fig. 6a. Karpenko et al. (2004ab) suggested the substitution  $(\text{SO}_4)^{2-} + \text{Al}^{3+} \leftrightarrow (\text{VO}_4)^{3-} + \text{Si}^{4+}$ , which leads to V–Si-bearing nickelalumite (analyses 13 and 14, Table 2). The complexity of the compositional variations involving (Ni, Zn), Al, V and S in nickelalumite–ankinovichite is apparent on the characteristic X-ray maps of those elements (Fig. 7).

### X-ray powder diffraction

X-ray powder diffraction data for nickelalumite were collected on a 57.3 mm RKD powder camera using Ni-filtered  $\text{CuK}\alpha$  X-radiation and the data are listed in Table 3. The pattern was indexed using the cell dimensions and measured reflection intensities from the single-crystal X-ray data. Unit-cell parameters refined from powder data are as follows:  $a = 10.219(10)$ ,  $b = 8.863(12)$ ,  $c = 17.103(15)$  Å,  $\beta = 95.26(10)^\circ$ ,  $V = 1543(2)$  Å<sup>3</sup>,  $Z = 4$ .

### Single-crystal X-ray data collection and refinement

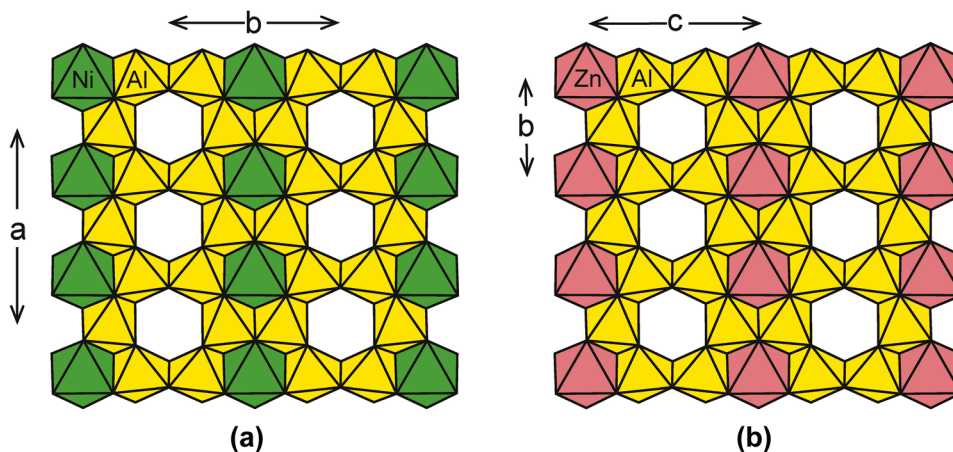
X-ray diffraction data for nickelalumite were collected with a Bruker P4 diffractometer equipped with a 4K CCD detector ( $\text{MoK}\alpha$  radiation) from a single-crystal of nickelalumite with dimensions  $0.10 \times 0.06 \times 0.02$  mm. The intensities of 7103 reflections with  $-10 < h < 10$ ,  $-9 < k < 9$ ,  $-18 < l < 18$  were collected to  $59.99^\circ 2\theta$  using 30 s per  $0.2^\circ$  frame: an empirical absorption correction (SADABS, Sheldrick 2008) was applied. The refined unit-cell parameters were obtained from 3365 reflections with  $I > 20\sigma I$ . There were no data in the region between  $59.99^\circ$  and  $45^\circ$ , and the data were truncated to  $44.42^\circ$ . The crystal structure of nickelalumite was solved using the Patterson method and refined to  $R_1 = 5.66\%$  and a GoF value of 1.059 for 1554 independent reflections (281 refined parameters including extinction) with the Bruker SHELXTL version 5.1 system of programs. Site occupancy

**Table 6** Refined site-scattering values (*epfu*) and assigned site-populations (*apfu*) for nickelalumite

	Refined site-scattering	Site population	Calculated site-scattering	$\langle X - \varphi \rangle_{\text{calc.}}^*$	$\langle X - \varphi \rangle_{\text{obs.}}$
<i>M</i>	27.63(15)	0.55Ni + 0.39Zn + 0.02V + 0.01Fe	27.82	2.089	2.079

\* Calculated by summing constituent ionic radii; values from Shannon (1976)

**Fig. 8** (a) The  $[\text{NiAl}_4(\text{OH})_{12}]$  sheet in nickelalumite and (b) the analogous  $[\text{ZnAl}_4(\text{OH})_{12}]$  sheet in alvanite. Ni octahedra: green; Al octahedra: yellow; Zn octahedra: orange



was refined for the  $M$  site (occupied primarily by Ni and Zn, plus minor V and Fe).

Details of the data collection and structure refinement are given in Table 4, details of hydrogen bonding in Table 5, and refined site-scattering values and assigned populations for selected sites are given in Table 6. Tables of final atom parameters and selected interatomic distances and angles are included in Supplementary Materials. Further details of data collection and structure refinement can be retrieved from the Crystallographic Information File (CIF), also included in Supplementary Materials.

## Crystal structure of nickelalumite

### Cation sites

There are five octahedrally coordinated sites in the nickelalumite structure. The  $M$  site is occupied by Ni and Zn with minor V and Fe:  $(\text{Ni}_{0.55}\text{Zn}_{0.39}\text{V}_{0.02}\text{Fe}_{0.01})_{\Sigma 0.97}$ ,  $\langle M\text{-OH} \rangle =$

2.079 Å. There are four sites occupied solely by Al, with  $\langle Al\text{-OH} \rangle = 1.900$  Å. There is one tetrahedrally coordinated  $S$  site with  $\langle S\text{-O} \rangle = 1.468$  Å. There are twelve anion sites occupied by (OH) groups and three sites fully occupied by ( $\text{H}_2\text{O}$ ). The refined and calculated site-scattering values and the observed and calculated  $\langle X\text{-}\varphi \rangle$  distances ( $\varphi =$  unspecified ligand) are in accord with the site populations in Table 6.

### Structure topology

In the nickelalumite structure, Al octahedra are connected through common edges to form six-membered rings with an octahedron at the centre of the ring. Half of these octahedra are occupied by Ni and Zn, and half are vacant.  $M$  and Al octahedra form a  $[(\text{Ni,Zn})\text{Al}_4(\text{OH})_{12}]^{2+}$  sheet parallel to (001) (Fig. 8a). The ( $\text{SO}_4$ ) tetrahedra and ( $\text{H}_2\text{O}$ ) groups occupy interstitial space between sheets of  $M\text{-Al}$  octahedra (Fig. 9a), and ( $\text{SO}_4$ ) tetrahedra link by hydrogen bonds involving donor O-atoms of ( $\text{H}_2\text{O}$ ) groups and acceptor O-atoms of ( $\text{SO}_4$ ) tetrahedra (Figs. 9a, 10a, Table 5).

**Fig. 9** Interleaved sheets of  $[\text{M}^{2+}\text{Al}_4(\text{OH})_{12}]$  and layers of  $\{(\text{TO}_4)_n(\text{H}_2\text{O})_m\}$  in (a) nickelalumite and (b) alvanite. Legend as in Fig. 8; ( $\text{SO}_4$ ) groups: mauve; ( $\text{VO}_4$ ) groups: pink; O atoms: pale-blue circles; H atoms: small red circles

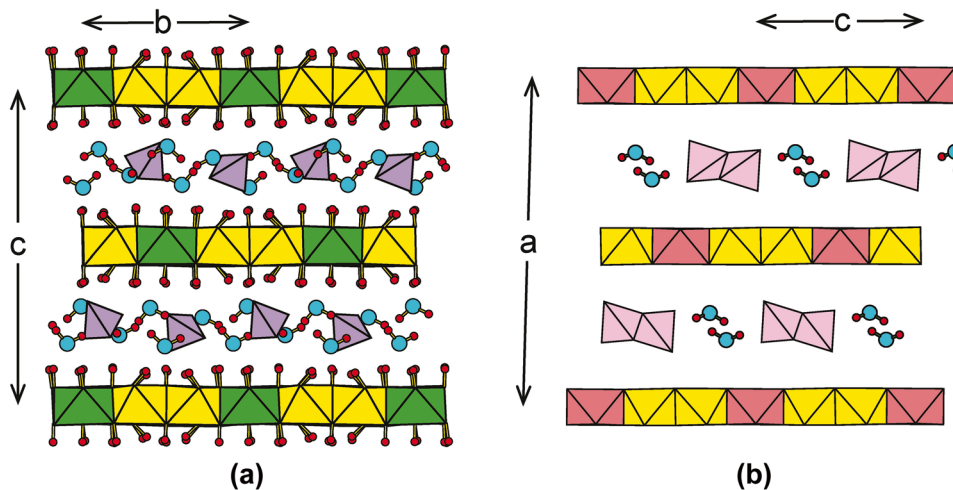


**Fig. 10** The interstitial layers in (a) nickelalumite and (b) alvanite. Legend as in Fig. 9; O<sub>w</sub>–H bonds are shown as solid black lines and hydrogen bonds are shown as dashed black lines

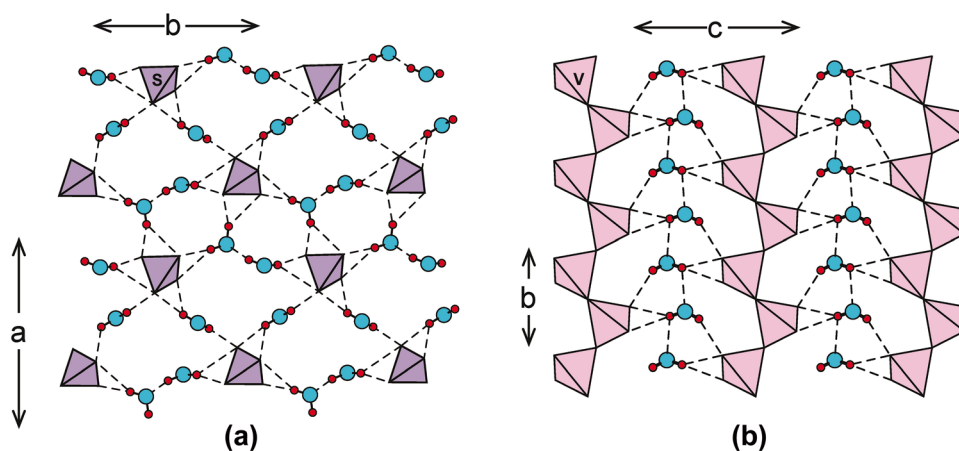


**Table 7** Comparison of data for nickelalumite, kyrgyzstanite, mbobomkulite, hydrombobomkulite, chalcoalumite, alvanite and ankinovichite

Mineral name	Ideal formula	Space group	<i>a</i> , Å	<i>b</i> , Å	<i>c</i> , Å	$\beta$ , °	Z	Ref.
Nickelalumite	NiAl <sub>4</sub> (SO <sub>4</sub> )(OH) <sub>12</sub> (H <sub>2</sub> O) <sub>3</sub>	<i>P2<sub>1</sub>/n</i>	10.2567(5)	8.8815(4)	17.0989(8)	95.548(1)	4	(1)
Kyrgyzstanite	ZnAl <sub>4</sub> (OH) <sub>12</sub> (SO <sub>4</sub> )(H <sub>2</sub> O) <sub>3</sub>	<i>P2<sub>1</sub>/n</i>	10.246	8.873	17.220	96.41	4	(2)
Mbobomkulite	(Ni,Cu <sup>2+</sup> )Al <sub>4</sub> [(NO <sub>3</sub> ),(SO <sub>4</sub> ) <sub>2</sub> ](OH) <sub>12</sub> (H <sub>2</sub> O) <sub>3</sub>	undetermined	10.171	8.865	17.145	95.37	4	(3)
Hydrombobomkulite	(Ni,Cu <sup>2+</sup> )Al <sub>4</sub> [(NO <sub>3</sub> ),(SO <sub>4</sub> ) <sub>2</sub> ](OH) <sub>12</sub> (H <sub>2</sub> O) <sub>12</sub>	undetermined	10.145	17.155	20.870	90.55	4	(3)
Chalcoalumite	CuAl <sub>4</sub> (SO <sub>4</sub> )(OH) <sub>12</sub> (H <sub>2</sub> O) <sub>3</sub>	<i>P2<sub>1</sub>/n</i>	10.228(3)	8.929(3)	17.098(6)	95.800(11)	4	(4)
Alvanite	ZnAl <sub>4</sub> (VO <sub>3</sub> ) <sub>2</sub> (OH) <sub>12</sub> (H <sub>2</sub> O) <sub>2</sub>	<i>P2<sub>1</sub>/n</i>	17.808(8)	5.132(3)	8.881(4)	92.11(3)	2	(5)
Ankinovichite	NiAl <sub>4</sub> (VO <sub>3</sub> ) <sub>2</sub> (OH) <sub>12</sub> (H <sub>2</sub> O) <sub>2</sub>	<i>P2<sub>1</sub>/n</i>	17.8098(8)	5.1228(2)	8.8665(4)	92.141(1)	2	(6)

References: (1) Uvarova et al. (2005); (2) Agakhanov et al. (2005); (3) Martini (1980); (4) Hawthorne and Cooper (2013); (5) Pertlik and Dunn (1990) (6) Karpenko et al. (2004b)

Hydrogen bonds link donor O-atoms of (OH)-groups to acceptor O-atoms of (H<sub>2</sub>O) groups and (SO<sub>4</sub>) tetrahedra (Figs. 9a, 10a) to link the [(Ni,Zn)Al<sub>4</sub>(OH)<sub>12</sub>] structural unit to the interstitial {(SO<sub>4</sub>)(H<sub>2</sub>O)<sub>3</sub>} layer.

### Relation to other structures

Nickelalumite has a stoichiometry (Table 2) similar to that of kyrgyzstanite: (Zn, Ni)(Al<sub>4</sub>(SO<sub>4</sub>)(OH)<sub>12</sub>(H<sub>2</sub>O)<sub>3</sub>, (Agakhanov et al. 2005), mbobomkulite:

(Ni, Cu<sup>2+</sup>)Al<sub>4</sub>[(NO<sub>3</sub>),(SO<sub>4</sub>)<sub>2</sub>](OH)<sub>12</sub>(H<sub>2</sub>O)<sub>3</sub>, hydrombobomkulite: (Ni,Cu<sup>2+</sup>)Al<sub>4</sub>[(NO<sub>3</sub>),(SO<sub>4</sub>)<sub>2</sub>](OH)<sub>12</sub>(H<sub>2</sub>O)<sub>12</sub> (Martini 1980) and chalcoalumite: CuAl<sub>4</sub>(SO<sub>4</sub>)(OH)<sub>12</sub>(H<sub>2</sub>O)<sub>3</sub> (Larsen and Vassar 1925; Williams and Khin 1971). The crystal structures of nickelalumite and kyrgyzstanite were solved by Uvarova et al. (2005) and Agakhanov et al. (2005), and the structure of chalcoalumite was eventually refined by Hawthorne and Cooper (2013) on a rotating-anode diffractometer. The similarity of the stoichiometries, cell dimensions and space groups of mbobomkulite and hydrombobomkulite (Table 7) suggest that the former is isostructural with chalcoalumite (the earliest named member of the group) and the latter has a related structure.

The crystal structure of nickelalumite involves a [NiAl<sub>4</sub>(OH)<sub>12</sub>] sheet (Fig. 8a) topologically identical to the analogous [ZnAl<sub>4</sub>(OH)<sub>12</sub>] sheet (Fig. 8b) in alvanite, ideally ZnAl<sub>4</sub>(VO<sub>3</sub>)<sub>2</sub>(OH)<sub>12</sub>(H<sub>2</sub>O)<sub>2</sub> (Pertlik and Dunn 1990), and ankinovichite NiAl<sub>4</sub>(VO<sub>3</sub>)<sub>2</sub>(OH)<sub>12</sub>(H<sub>2</sub>O)<sub>2</sub> (Karpenko et al. 2004b). In the structure of nickelalumite, [NiAl<sub>4</sub>(OH)<sub>12</sub>] sheets are connected through isolated (SO<sub>4</sub>) tetrahedra and (H<sub>2</sub>O) groups (Figs. 9a, 10a) whereas in alvanite and ankinovichite, layers of octahedra are linked by hydrogen bonds to unbranched [TO<sub>3</sub>] chains (Figs. 9b, 10b), a very common linkage of tetrahedra in minerals (Day and Hawthorne 2020, 2022). The differences between the nickelalumite-type structure and the alvanite-type structure are best shown by their interstitial layers (Fig. 10). In the nickelalumite structure, sulfate tetrahedra are linked by hydrogen bonds involving interstitial (H<sub>2</sub>O) groups (Figs. 9a, 10a), whereas in the alvanite structure, [VO<sub>3</sub>]<sup>1-</sup> chains of tetrahedra link *via* hydrogen bonds involving chains of hydrogen-bonded (H<sub>2</sub>O) groups (Figs. 9b, 10b). The different two-dimensional packing arrangements of these two interstitial layers accounts for the different content of (H<sub>2</sub>O) in each structure type: (H<sub>2</sub>O)<sub>3</sub> in nickelalumite (Fig. 10a) and (H<sub>2</sub>O)<sub>2</sub> in alvanite (Fig. 10b).

**Supplementary Information** The online version contains supplementary material available at <https://doi.org/10.1007/s00710-023-00832-3>.

**Acknowledgements** We thank Vladimir M. Rogovoy, Vladimir N. Bobylev, Vasilii S. Gurskii and Vladimir V. Smirnov for help during field work. We are grateful to Ilya B. Afanasyev for his help in obtaining BSE images of nickelalumite crystals, to Nikita V. Chukanov for discussion of the Raman spectra, and to Natalya A. Pekova for obtaining the macrophoto of nickelalumite spherulites from Kara-Chagyr. We are particularly grateful to Daniel Bernardo (Council for Geoscience South Africa) for help in obtaining a sample of nickelalumite from the National Museum of Natural History (Pretoria, RSA) and to Jacques Martini for detailed information concerning investigation of minerals from the Mbobomkulu cave. We are grateful to two anonymous reviewers, Guest Editor Manfred Wildner, and Editor-in-Chief Lutz Nasdala for their comments and help in producing the final paper. Financial support for this work came from the Natural Sciences and Engineering Research Council of Canada in the form of a Canada Research Chair in Crystallography and Mineralogy, and a Discovery grant to FCH, and by Canada Foundation for Innovation grants to FCH.

## References

- Agakhanov AA, Karpenko VYu, Pautov LA, Uvarova YA, Sokolova E, Hawthorne FC, Bekenova GK (2005) Kyrgyzstanite,  $\text{ZnAl}_4(\text{SO}_4)(\text{OH})_{12}(\text{H}_2\text{O})_3$  – a new mineral from the Kara-Tangi, Kyrgyzstan. *New Data on Minerals* 40:23–28
- Bartelmehs KL, Bloss FD, Downs RT, Birch JB (1992) Excalibr II. *Z. Kristallogr* 199:185–196
- Day MC, Hawthorne FC (2020) A structure hierarchy for silicate minerals: Chain, ribbon, and tube silicates. *Mineral Mag* 84:165–244
- Day MC, Hawthorne FC (2022) Bond topology of chain, ribbon and tube silicates. Part I. Graph- theory generation of infinite one-dimensional arrangements of  $(\text{TO}_4)^n$  tetrahedra. *Acta Crystallogr A* 78:212–233
- Hawthorne FC, Cooper MA (2013) The crystal structure of chalcoalumite: mechanisms of Jahn-Teller-driven distortions in  $^{16}\text{Cu}^{2+}$ -containing oxysalts. *Mineral Mag* 77:2901–2912
- Jarosewich E (2002) Smithsonian microbeam standards. *J Res Natl Inst Stan Technol* 107:681–685
- Karpenko VYu, Agakhanov AA, Pautov LA, Dikaya TV, Bekenova GK (2004a) New occurrence of nickelalumite on Kara-Chagyr, South Kirgizia. *New Data on Minerals* 39:32–39
- Karpenko VYu, Agakhanov AA, Pautov LA, Sokolova E, Hawthorne FC, Dikaya TV, Bekenova GK (2004b) Ankinovichite, nickel analogue of alvanite, a new mineral from Kurunsak (Kazakhstan) and Kara-Chagyr (Kirgizia). *Zap Vses Mineral Obschest* 133(2):59–70 ((in Russian))
- Karpenko VYu, Pautov LA, Agakhanov AA (2009) Discovery of low aluminium nevadaite from the Kara Chagyr area, Kyrgyzstan. *Geology of Ore Deposits* 51:794–799
- Karpenko VYu, Pautov LA, Agakhanov AA, Bekenova GK (2011) On mannardite from vanadium-bearing schists of Kazakhstan and Central Asia. *New Data on Minerals* 46:25–33
- Karpenko VYu, Pautov LA, Agakhanov AA (2016) About Ni-Zn-bearing volborthite (“uzbekite”) from vanadium-bearing schists of Southern Kyrgyzstan. *New Data on Minerals* 51:20–29
- Larsen ES, Vassar HE (1925) Chalcoalumite, a new mineral from Bisbee, Arizona. *Am Mineral* 10:79–83
- Martini JEJ (1980) Mbobomkulite, hydrombobomkulite, and nickelalumite, new minerals from Mbobomkulu cave, eastern Transvaal. *Ann Geol Surv S Afr* 14:1–110 (reference obtained from *Am Mineral* 67:415–416, 1982)
- Merlet C (1992) Quantitative electron probe microanalysis: new accurate  $\Phi(\rho z)$  description. *Mikrochim Acta* 12:107–115
- Pertlik F, Dunn PJ (1990) Crystal structure of alvanite,  $(\text{Zn,Ni})\text{Al}_4(\text{VO}_3)_2(\text{OH})_{12}\bullet 2\text{H}_2\text{O}$ , the first example of an unbranched zweier-single chain vanadate in nature. *Neues Jb Mineral Monat* 385–392
- Porshnyakov GS, Kotov NV, Kol'tsov AB, Vaganov PA, Zakharevich KV, Zubtsov SYe, Donskikh AV, Nesterov AR, Poritskaya LG (1991) Geological position and petrological and geochemical features of gold ore metasomatites in black shale strata. *DVO AN SSSR, Vladivostok*, 47 pp ((in Russian))
- Preobrazhensky IA (1926) Deposits of radioactive minerals in Western Fergana. *Proceedings on the study of radium and radioactive ores II:73–120* ((in Russian))
- Scherbakov DI (1924) Deposits of radioactive ores and minerals of the Fergana and tasks for their further investigation. *Reports for Studies of Natural Productivity Forces* 47:1–9 ((in Russian))
- Shannon RD (1976) Revised effective ionic radii and systematic studies of interatomic distances in halides and chalcogenides. *Acta Crystallogr A* 32:751–767
- Sheldrick GM (2008) A short history of SHELX. *Acta Crystallogr A* 64:112–122
- Uvarova YA, Sokolova E, Hawthorne FC, Karpenko VYu, Agakhanov AA, Pautov LA (2005) The crystal chemistry of the “nickelalumite”-group minerals. *Can Mineral* 43:1511–1519
- Williams GR, Moorehouse SJ, Prior TJ, Fogg AM, Rees NH, O’Hare D (2011) New insights into the intercalation chemistry of  $\text{Al}(\text{OH})_3$ . *Dalton Trans* 40:6012–6022
- Williams SA, Khin BS (1971) Chalcoalumite from Bisbee, Arizona. *Mineral Rec* 2:126–127

**Publisher's Note** Springer Nature remains neutral with regard to jurisdictional claims in published maps and institutional affiliations.

Springer Nature or its licensor (e.g. a society or other partner) holds exclusive rights to this article under a publishing agreement with the author(s) or other rightsholder(s); author self-archiving of the accepted manuscript version of this article is solely governed by the terms of such publishing agreement and applicable law.